IJE TRANSACTIONS A: Basics Vol. 36 No. 07, (July 2023) 1331-1342

International Journal of Engineering

Journal Homepage: www.ije.ir

Power and Ventilation Performance Study in a Modified Vertical Axis Wind Turbine Based on Semi-analytical Approach

S. Karimian*, S. Saham

Mechanical Faculty, Tarbiat Modares University, Tehran, Iran

P A P E R I N F O

Paper history:
Received 14 January 2023
Received in revised form 09 April 2023
Accepted 15 April 2023

Keywords:
Wind Energy Potential
Modified Vertical Axis Wind Turbine
Double Multiple Stream Tube Method
Power Coefficient
Ventilation Coefficient

A B S T R A C T

In the current research, a novel vertical axis wind turbine producing both power and ventilation is presented. The idea is similar to an ancient wind catchers. The wind capacity of the Manjil city in Iran has been studied and a typical home-scale wind turbine has been assessed. To modify the geometry, a 3D semi-analytical code has been developed based on Double Multiple Stream Tube (DMST) theory. The validation analysis has been accomplished by the reference turbine. Using this code, the turbine performance including power coefficient and flow diversion index was studied. Particularly the effect of blade cone angle on the power deficiency and ventilation ratio was investigated. The results of the parameter study would reveal that for the optimal range of tip speed ratio, 2.9-3.2 based on the power curve, it is feasible to produce up to 400 m^3/h ventilation flow and 50-200 W shaft power. It would be obtained by 20-degree blade inclination and is equivalent to 2.5% of the total flow entering the rotor. The power deficiency due to this change is 30% which is compromised by the ventilation capability. The results also revealed the optimal range of tip speed ratio is 2.9-3.2. . It is depicted that, power attenuation could be minimum when the suitable TSR and the appropriate geometry are selected. Finally, some generalized trends of the objective functions also have been drawn. The methodology is versatile for the ongoing problems in the field of vertical axis wind turbines.

***doi**: 10.5829/ije.2023.36.07a.14*

NOMENCLATURE

a	Induction factor	$\dot{m}$	Mass flow rate
V_∞	Wind speed	Q	Local torque
V_e	Induced equilibrium velocity	$\bar{Q}$	Mean torque
V_n	Normal velocity	$C_{\bar{Q}}$	Mean torque coefficient
V_t	Tangential velocity along the blade chord	C_P	Power coefficient
V_s	Tangential velocity along the blade length	C_L	Lift coefficient
W	Relative velocity	C_D	Drag coefficient
V_z	Velocity along the rotor axis	L	Lift
V_a	Axial induction velocity	D	Drag
C_n	Normal force coefficient	r	The local radius of the rotor
C_t	Tangential force coefficient	Δz	Blade element height
f	Blade function	B	Number of Blades
N	Normal force	**Greek Symbols**	
T	Tangential force	λ	Tip speed ratio
c	Blade chord	ω	Rotating speed
A	Swept area	α	Angle of attack
		η	Non-dimensional blade length

1. INTRODUCTION

The growth of science, technology, and industries, as well as the increase in population and the need for extra energy, has led to the world dealing with environmental problems and renewable energy sources. Wind turbines are one of the best ways to supply green energy as they are cost-effective and environmentally friendly. It is

*Corresponding Author Institutional Email: karimian@modares.ac.ir
(S. Karimian)

Please cite this article as: S. Karimian, S. Saham, Power and Ventilation Performance Study in a Modified Vertical Axis Wind Turbine Based on Semi-analytical Approach, ***Journal of Engineering, Transactions A: Basics***, Vol. 36, No. 07, (2023), 1331-1342

estimated that they can provide more than 20% of the world's energy demand [1]. Wind turbines come in different dimensions and types and can be installed in various sites from wind farms to rooftops. Wind energy systems also have a wide variety of components such as wind turbines, vibration absorbers, airborne systems, and flapping mechanisms. Wind turbines can be classified into two types: horizontal axis and vertical axis. Horizontal axis turbines have more power but require more investment and space. Vertical axis wind turbines (VAWTs) have several key advantages, including smaller dimensions, insensitivity to wind direction, and lower construction and service costs. VAWTs are suitable for installation in workshops, roofs, highways, and urban thoroughfares.

Iran is located in a low-pressure region that is affected by strong summer and winter currents originating from the Atlantic and Indian Oceans. Studies on Iran's wind potential have been conducted in the southeastern regions, including Zahedan, and the northern regions, including Manjil. Iran's first experience of producing industrial wind energy was achieved by installing a series of 500 kW wind turbines in Manjil and Rudbar in 2015, providing 1800 MW.h energy per year [2]. While the wind potential for using large scale horizontal axis wind rotors in Iran has been frequently studied, this article focuses on vertical axis turbines due to their lower cost, versatility, and suitability for small scale wind systems. The article reviews several new works dealing with Iran's wind potential and presents recent literature on related VAWT studies. Alamdari et al. [3]compared wind speeds at altitudes of 10, 30, and 40 meters above the ground in different climates across Iran. They estimated the average and distribution functions, as well as the probability density function, using data from 68 stations [3]. Mostafaeipour [4] studied wind energy feasibility in the Yazd region, measuring wind speeds monthly and annually at various altitudes between 1992 and 2005 at 11 meteorological stations. In another study, researchers evaluated the economic potential of small wind turbines in Kerman. They examined three small turbines and demonstrated that the region has potential for wind energy utilization [5]. Many researchers have explored the potential of wind energy in various regions of Iran, such as Kerman and Manjil [6], and compared it with regions in Germany [7], Turkey [8], and Greece [9, 10].

In 2009, Paraschivoiu et al. [11] analyzed the performance of a vertical axis wind turbine with pitch angle control capabilities using the coupling method of the genetic algorithm with the DMST model. Their study focused on the performance and pitch control mechanism of the H-shaped turbine. The results showed that continuous pitch angle control has a relatively better performance than sinusoidal control and can increase turbine power by about 30% annually [11]. In 2017, Cheng et al. [12] compared the results of a two-dimensional study and three-dimensional simulation of a vertical axis wind turbine with helical blades using the LES and RANS methods. They found that changes in the angle of attack and the wake created across the rear blade had a significant effect on the turbine power coefficient. They also observed that the tip vortices of the blade were one of the effective factors in power and noise factors in the three-dimensional simulation [12]. In 2018, Zanforlin and Deluca [13] examined the effects of Reynolds number and blade tip loss factor on the performance of a vertical axis wind turbine with straight blades. They found that both factors could affect turbine performance, with the effect of blade tip loss being predominant in medium and large turbine sizes and the Reynolds number effect being greater in small turbines [13].

Rasekh et al. [14] in 2018 examined dynamic stall in the wind turbine blade and used two models, the Leishman-Beddoes semi-analytical dynamic stall and the numerical method. They compared results and revealed that dynamic stall in both methods depended on factors such as the initial and mean angle of attack, reduced frequency, and phase angle. They also observed that the Leishman-Beddoes method would have acceptable results with less computational cost. In 2021, Karimian and Rasekh [15] discussed the relation between power performance, acoustics, and geometry of a vertical axis turbine. They found that implementing some small changes in blade pitch angle could effectively enhance the power coefficient, with the greatest effect occurring at a low tip speed ratio. They also observed that small changes in pitch angle could reduce undesirable noise, especially at low turbine speed ratios [15].

In 2019, Moghimi and Motawej [16] used the DMST method to study the aerodynamic performance of H-rotor turbines and Gorlov turbines. They examined the impact of various geometric parameters, including airfoil shape and chord, number of blades, helix angle, wind speed, and aspect ratio. The researchers concluded that thicker airfoils with longer chords were more suitable for turbine operation. Utilizing fewer blades, shorter chord lengths, and smaller aspect ratios can cover a wider range of tip speed ratios. They also claimed that the helical angle of the blade has little effect on the power coefficient, although it was expected to reduce torque oscillations [16]. In 2014, Sedaghat et al. [17] investigated a horizontal axis wind turbine with a continuous change in wind speed. They improved the BEM method by generalizing the quadratic equations about the angular induction factor. The researchers also determined the optimal point of turbine operation in terms of maximum power coefficient and maximum lift-to-drag ratio. Finally, they stated that using a turbine with a continuously variable speed has a higher power coefficient than conventional constant-speed wind turbines [17]. In 2015, Sedaghat et al. [18] attempted to achieve a higher lift-to-drag ratio by circulating the

turbine blades. They were able to achieve a lift-to-drag coefficient of 278 by applying this change and utilizing the Magnus effect. The researchers stated that this was true for a wide range of symmetrical airfoils [18].

Liu and Mak [19] investigated windcatchers in 2007, examining the impact of wind speed and direction. They found that the wind speed entering the windcatcher was approximately equal to the free wind speed in the environment, which created suitable conditions for ventilation. They also observed that as wind speed increased, the flow rate through the windcatcher could be expedited by utilizing a small azimuth angle between 5-15 degrees. However, increasing this azimuth angle could decrease the flow rate through the windcatcher. They also noted that in cases of higher wind velocity or larger angles, the uniformity of the flow entering the wane would be decreased [19].

In 2017, Chong et al. [20] introduced a cross-axis wind turbine design that used three vertical-axis blades and six horizontal-axis blades perpendicular to each other. They also used additional blades to divert the flow and installed them in the rotor plan of the horizontal-axis turbine blades. This design allowed the vertical-axis turbine blades to operate initially, followed by the horizontal-axis turbine blades, improving turbine performance [20]. While Iran has suitable windy areas, its contribution to the use of wind energy is still below average due to cheap fossil fuel energy resources in the Middle East hindering the development of large-scale wind farms and high-power offshore horizontal axis turbines. Therefore, it is more attractive and effective to use wind energy in domestic and urban applications, focusing on small and medium-sized vertical-axis turbines. These turbines can be more efficient and effective on an urban scale, achieving economic and environmental benefits. Adanta et al. [21] in 2023, conducted a study to optimize a pico-hydro-type crossflow turbine's performance by curving the upper surface of the blade and increasing the lift force. Their numerical solution results revealed that the upper CFT blade has a parabolic effect on the turbine's performance and specific speed. They recommended that a CFT with a curved blade is generally more suitable for low-pressure conditions with extreme fluctuations [21].

The central idea and innovation of this study is to combine the power generation index with the home air-conditioning concept. By using angled blades in the vertical-axis turbine, it is possible to divert the output current from the turbine in addition to power generation. After evaluating the wind energy potential in Manjil as a sample area, the power and ventilation characteristics of a V-shaped turbine with proposed dimensions and geometry were investigated, and the effect of cone angle on turbine performance and flow rate was examined assuming a separating baffle. The researchers developed a semi-analytical code based on the DMST method and made some corrections, which is another achievement of this study. The steps for analyzing and evaluating the desired turbine are shown in Figure 1.

2. BASIC EQUATIONS AND MODELING

In this research, the analysis of the turbine is conducted based on the DMST method, which is implemented in MATLAB software. The momentum theory forms the foundation of this method, where the turbine rotor is divided into upwind and downwind semi-cycles, and the momentum equations of the flow are applied separately to each phase. The DMST method used in this study is an analytical method that offers the important advantage of quickly obtaining accurate results. Other similar methods include SST and MST. The DMST method outperforms similar analytical methods since it incorporates two operating discs and considers correction factors such as the Prandtl's factor. Figure 2 illustrates the division of the turbine rotor into stream tubes along the flow direction, with the azimuth angle $\Delta\theta$ corresponding to the segmentation of the stream tubes. When the free stream strikes the rotor blades upwind, it loses a part of its energy, and the velocity reduces to V_e. Similarly, the velocity V_e reduces due to the downwind blades' passage. Eventually, the flow leaving the rotor reaches its minimum velocity, V_w. The velocities at the upwind and downwind sections are abbreviated as V_{au} and V_{ad}, respectively, and are affected by the induction factors in the upwind and downwind strokes [22]. These factors represent the effect of blade wake history on the current flow passing through the rotor, and they can be computed iteratively using the momentum equations in two actuator discs, upwind and downwind.

$$V_\infty > V_{au} > V_e > V_{ad} > V_w \quad (1)$$

$$V_{au} = a_u V_\infty \quad (2)$$

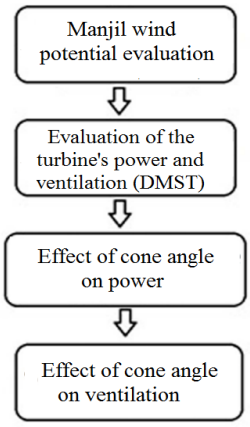

Figure 1. Evaluation of the V-shaped wind turbine structure

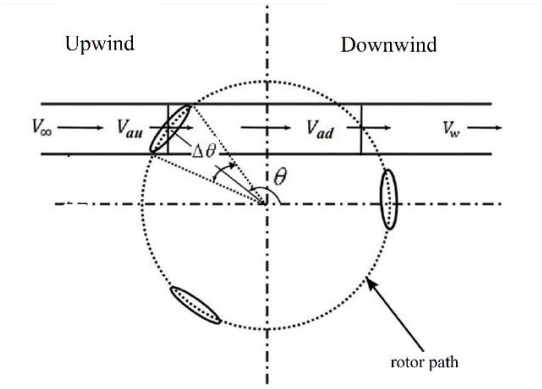

Figure 2. One typical Stream-tube used in the DMST method [22]

$$V_e = V_\infty(2a_u - 1) \quad (3)$$

$$V_{ad} = a_d V_e \quad (4)$$

Initially assuming some values for the induction factor a, the flow velocity can be calculated in the desired section. Relative flow velocity is crucial in estimating aerodynamic performance, the instantaneous relative velocity and the corresponding apparent angle of attack are determined by Equations (5) and (6) [19]. Figure 3 illustrates the position of a specific blade at four different moments during one cycle, demonstrating considerable variation in the magnitude and direction of the relative velocity and angle of attack. Using the prior quantities to obtain the lift and drag forces, one can easily determine the tangential and perpendicular force components. Figure 4 shows the DMST algorithm. Because the turbine blades have a finite length, some flow at the tip of the blade is diverted from the high-pressure surface to the low-pressure surface, causing blade tip vortices. These tip vortices generate a downwash flow and change the relative velocity vector, leading to a reduction in the effective angle of attack, particularly at the blade's tip, decreasing aerodynamic performance.

To improve the DMST method, Prandtl's tip loss factor correction is used, based on Equation (8). The 3D-lift coefficient and induced drag are determined according to Equations (7) to (9). The parameters η and α represent the nodal non-dimensional spanwise position and geometric angle, respectively [22].

$$W = \sqrt{(V_n)^2 + (V_t)^2 + (V_s)^2} \quad (5)$$

$$\alpha = \sin^{-1}(V_n/W) \quad (6)$$

$$f = N/2\,((1-\eta)/(\eta\,\sin|\alpha|)) \quad (7)$$

$$C_{L(3D)} = C_{L(2D)}(2/\pi)\cos^{-1}\left(e^{-f}\right) \quad (8)$$

$$C_{D(ind)} = \left(C_{L(3D)}^2/(0.95\pi.AR)\right) \quad (9)$$

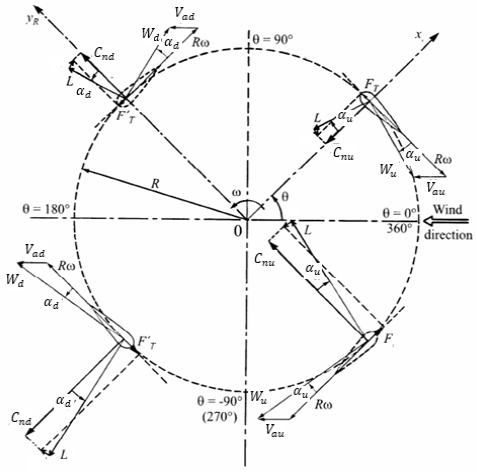

Figure 3. Flow angle, forces, and velocity vector [22]

Moving on to the next step, the lift and drag coefficients are estimated. The normal and tangential force coefficients can be computed. Once the force coefficients are obtained, the force magnitudes in each section can be determined according to Equations (10) and (11) [22]. In these equations, ρ is the air density, c is the blade chord, Δh is the blade element increment, W is the relative flow velocity, and C_n and C_t are the normal and tangential force coefficients, which are transformed by the lift and drag coefficients. By calculating the normal and tangential force coefficients, the new estimation of the induction factor can be obtained using Equations (12) and (13) [22].

$$F_N(\theta) = \left(\frac{1}{2}C_n.\rho.c.\Delta h.W^2\right) \quad (10)$$

$$F_T(\theta) = \left(\frac{1}{2}C_t.\rho.c.\Delta h.W^2\right) \quad (11)$$

Consequently, the new approximations of relative flow velocity, angle of attack, and normal and tangential force coefficients are determined. The loop is repeated for each element of the blade and each azimuth angle until convergence is achieved. It is notable that the induction factor iterations are different upwind and downwind and must be examined separately. The final values of normal and tangential forces on each blade section can then be integrated to calculate the total forces applied to the entire turbine. One of the most interesting components of the total force is the one parallel to the turbine axis (z-direction of the fixed coordinate axis).

According to the simple momentum theory, the downward flow velocity and the related discharge rate ($\dot{V}$) can be predicted using Equations (14) and (15).

$$f = \frac{Bc}{8\pi r}\int_{-\pi/2}^{\pi/2}\left(C_n\frac{\cos\theta}{|\cos\theta|} - C_t\frac{\sin\theta}{|\cos\theta|\cos\delta}\right)\left(\frac{W}{V_a}\right)^2 d\theta \quad (12)$$

$$a_{new} = \pi/(f+\pi) \quad (13)$$

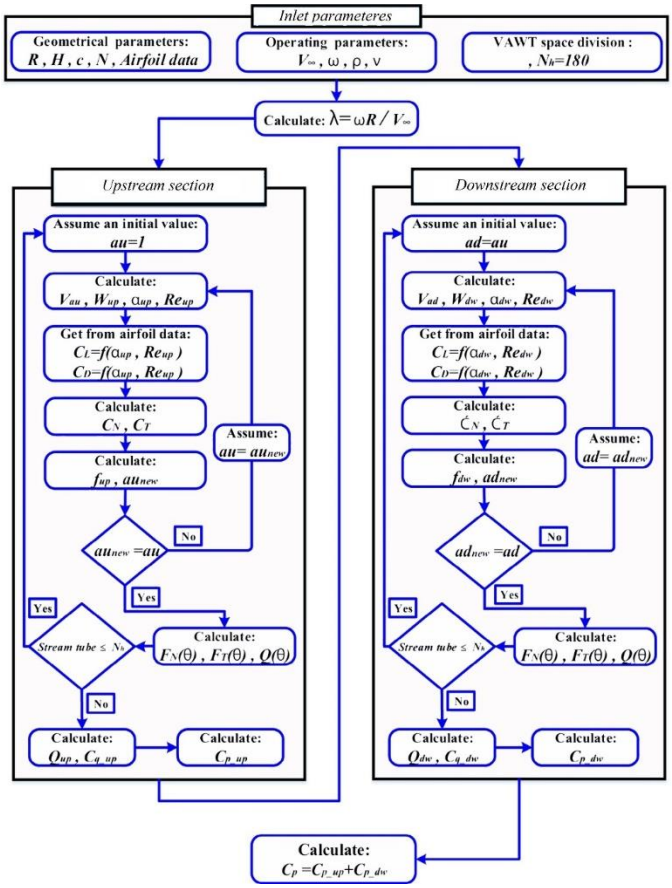

Figure 4. DMST algorithm [16]

$$V_z = \sqrt{\left(F_N \sin\delta\right)\cos\theta/\rho.A} \quad (14)$$

$$\dot{V} = A.V_z \quad (15)$$

In the subsequent step, Equation (16) to (18) are used to obtain the torque due to the tangential force and the turbine power [19]. The parameter $\bar{Q}$ represents the rotor's average torque and the parameter λ represents the blade tip speed ratio.

$$\bar{Q} = \frac{N}{2\pi}\int r.F_T(\theta)\,d\theta \quad (16)$$

$$C_P = \lambda.C_{\bar{Q}} \quad (17)$$

$$P = \frac{1}{2}\rho V^3 C_P \quad (18)$$

The DMST algorithm is based on the upwind and downwind computation of the rotor. To initialize the process, some input variables such as blade length, rotor diameter, blade chord, airfoil type, rotational speed, and free wind speed must be defined and set. Then, the blade is discretized, and the azimuth angles are divided, which can affect the accuracy of the method. After calculating the tip speed ratio for blade elements, one can proceed to the next step, i.e., the calculations related to the upwind of the rotor. In this step, the induction factor is scheduled to be found, as mentioned before. It may be accomplished by trial and error and by applying some default values for the induction factor. When the appropriate induction factor is obtained, key parameters of aerodynamic performance, such as relative speed and effective angle of attack, can be calculated.

By calculating the relative velocity and angle of attack, as well as the airfoil lift and drag coefficients, the blade's normal and tangential forces are calculated. Then, with proper transformation, the forces applied to the blade can be obtained, which include three force components: (1) in the direction of wind speed (x-axis), (2) perpendicular to the wind speed (y-axis), and (3) parallel to the turbine axis direction (z-axis). The torque applied to the blade is also calculated. The same process as for the upwind is repeated for the downwind stroke. The main difference is the lower inlet flow velocity. This intermediate velocity (V_e) is derived as stated at the beginning of this section. Finally, the velocity of the

downward flow parallel to the z-axis and the corresponding discharge is being estimated. This issue is addressed by ventilation capacity in the subsequent sections. Similar to the moment formula, the power extracted in upwind and downwind strokes will be estimated separately, and the overall performance can be achieved.

3. BASELINE TURBINE AND VENTILATION OF SEMI-ANALYTICAL CODE

To validate the method, an H-type turbine suitable for urban and home scales, with geometric characteristics are summarized in Table 1. The power coefficient obtained from the proposed method and implemented code is compared with both experimental data given by Castelli et al. [23] and numerical analysis are given by Mohamed [24]. As depicted in Figure 5, the horizontal axis represents the blade tip speed ratio, and the vertical axis represents the turbine power coefficient.

According to this figure, it can be seen that the DMST method presented in this study could appropriately estimate the power coefficient of the baseline turbine within a 14% relative error, which is acceptable when experiencing separation and complex wake interactions.

By evaluating the proposed model, the baseline H-type turbine (Figure 6) has been modified to meet both power and flow diversion objectives. Applying a conical angle would make the blade inclined concerning the turbine axis, resulting in a V-type turbine similar to

TABLE 1. characteristics of basic turbine [23]

Airfoil type	NACA 0021
Number of blades	3
Blade chord	0.08 m
Blade height	1.5 m
Rotor diameter	1 m

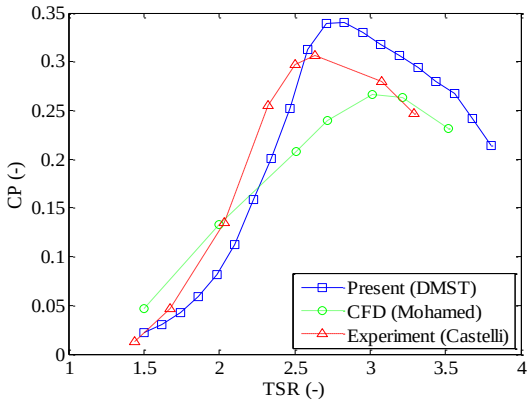

Figure 5. DMST method validation

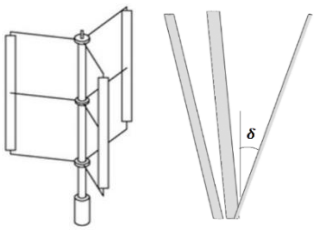

Figure 6. Baseline and modified V-type turbine ($\delta = 20^{\circ}$)

Figure 6. Assessing the wind energy potential of Manjil city, the V-type turbine will be modeled via the proposed DMST code, and its power and ventilation performance will be examined. The appropriate range of turbine operation in terms of production power and ventilation capacity is based on the presented parametric study.

Case study: Manjil city wind energy potential

Manjil, a city with a population of about 20,000 in Gilan province in northern Iran, is one of the most promising locations for wind energy in the country. The city experiences its strongest winds during spring and summer, which are commonly referred to as the "seven days Manjil winds." The establishment of different pressure patterns in the area is one of the reasons for the strong winds. This has resulted in one of the most robust local winds in the south of Caspian Sea. Additionally, the Sefidrood valley acts as a communication channel between Caspian Sea in the north and the vast land of Central Iran in the south. The difference in latitude and climate between these two zones results in significantly different conditions in air circulation patterns, pressure distribution, and temperature profiles. This leads to a massive rate of air exchange between Caspian Sea and the central land of Iran, although the Alborz mountain prevents it from being sustained continuously.

Figure 7 displays the average wind speed profile for Manjil city between 2018 and 2020. The city has an average speed of 9.5 m/s at a height of 10 meters, with the highest average speed of 15.9 m/s occurring in July and the lowest average speed of 4.5 m/s recorded in February. Figure 8 shows the frequency/probability distribution of the realized wind speed. The turbine design is proportional to the higher wind speed and the probability of occurrence of that high wind speed. The range of wind speed considered is 8 to 10 m/s. Based on the wind speed characteristics of Manjil, the maximum available power and annual wind energy of this site can be estimated as follows:

4. TURBINE VENTILATION AND POWER PERFORMANCE

In the preceding section, examined the available power in Manjil city. As previously mentioned, the main

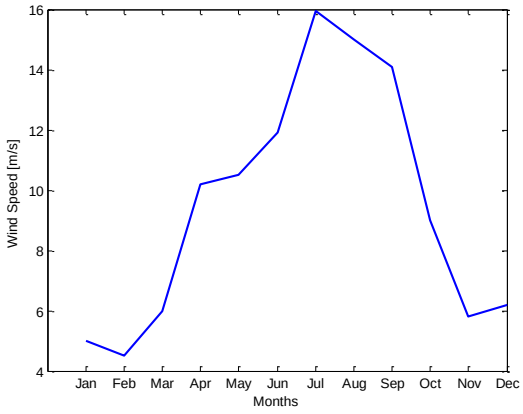

Figure 7. Average wind speed in Manjil [7]

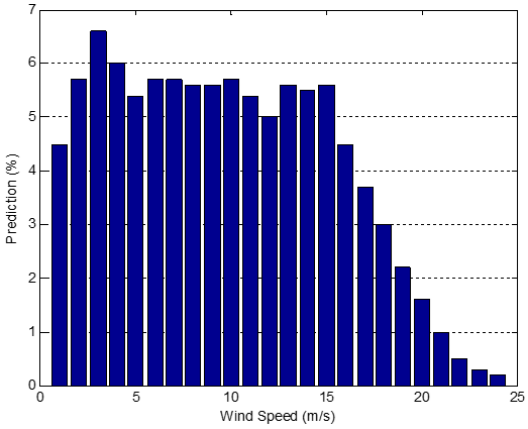

Figure 8. Wind speed histogram of Manjil [7]

concept is to combine the performance of old windcatchers used in desert areas of Iran with vertical axis turbines. The operation of the windcatcher can be described based on the principle of suction and discharge flow or based on the temperature difference. To build a similar mechanism, fresh air must first enter the room, and then hot and polluted air must be expelled from the room. By installing a V-shaped turbine on the roof of houses and placing a partition wall or baffle, as shown in Figure 9, it is possible to separate the supply flow from the stair flow.

Utilizing suitable V-rotor turbine, one may achieve both power generation and ventilation in a confined location. The airflow entering the upwind phase of the rotor will be partially diverted along the z-axis and used to create the inflow channel, which supplies fresh air. After circulating inside the room, it will be drawn out by the downwind phase of the turbine, which creates a suction flow in the upward z-direction. The fresh air and stale air channels are separate in order circulation occurred. They would not be mixed but are placed next to each other.

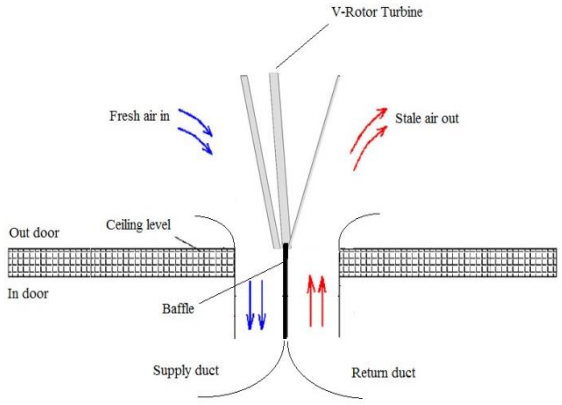

Figure 9. Schematic of the location of turbine and supply and return ducts of ventilation

Applying a conical angle on the base turbine is beneficial due to its flow-diverting and ventilation capability, but it will affect the output power of the turbine. Figure 10 shows that two cone angles of 10 and 20 degrees were applied, which caused the output power of the turbine to decrease. As the conical angle increased, the maximum extracted power decreased, but the slope of the power curve was smoothed, indicating a more extended range of wind speeds. This power reduction can be attributed to the reduction in the effective blade height and ultimately the reduction in the swept area by the rotor. Additionally, power loss at higher wind speeds decreases with increasing cone angle. In other words, the output power sensitivity to velocity change is attenuated.

The power coefficient representation based on the corrected reference area is shown in Figure 11. It can be observed that by applying the cone angle, the optimum tip speed ratio corresponding to the maximum power coefficient would be slightly increased. It still occurs within the proximity of a tip speed ratio equal to 3. By applying cone angle, the turbine would enter the stall at

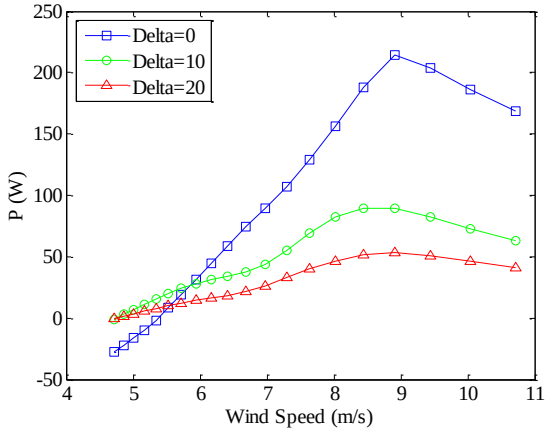

Figure 10. Effect of cone angle on the turbine power curve

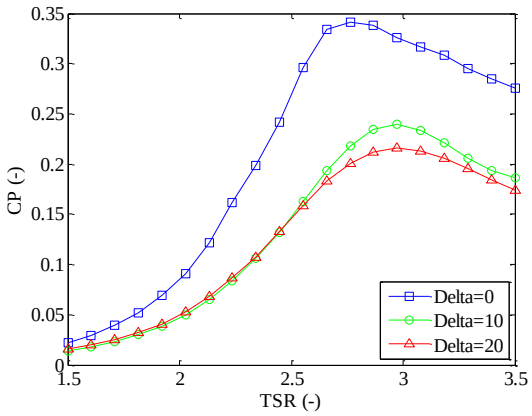

Figure 11. Effect of cone angle on turbine power coefficient curve

lower wind velocities. From the power point of view, the power would be decreased by the V-rotor configuration, but the sensitivity of the power coefficient is revealed to be enhanced.

By calculating the ventilated flow in the upwind and downwind of the rotor separately, it is possible to study the diversion flow performance. For conical angles of 0, 10, and 20 degrees, it is computed independently and shown in Figure 12. As it is seen the upwind values are negative (lower curves) due to the z-axis direction and the downwind values are positive (upper curves). According to the figure, it can be founded the amount of flow diverted as ventilation flow is directly related to wind speed and cone angle. Although increasing the wind speed and cone angle will increase the ventilation flow, but the trend is nonlinear. On the other hand, the sensitivity of discharged flow to the cone angle is shown to be gradually decreased. For example, it can be seen that the amount of flow diverted in D=20 is slightly greater than D=10, while the difference in diverted flow between D=0 and D=10 is definitely more. Increasing the wind speed would increase the amount of ventilation, except for the Stall case which causes a sharp drop in aerodynamic performance.

The axial flow velocity is depicted in Figure 13. As can be seen, the free-stream velocity is different in the upwind and downwind, concluding the stall velocity in both regions to be different. So the upwind rotor blades would experience a stall at lower wind speeds, while the downwind blades would encounter a stall at higher wind speeds. This result together with Figure 12, could explain why the downwind curves are asymptotic. The amount of ventilation in the downwind phase is initially increasing within a range up to 7 m/s with a relatively high slope. After that, the blades would enter the stall region, and consequently flow enhancement would be attenuated. The same profile would occur in the upwind, except that the stall velocity for upwind is less (about 5 m/s). The low TSR can be considered equivalent to a higher wind speed at a constant rotational speed. Therefore, in this TSR, the blades of the turbine would face with higher speed flow, causes the wind flow coming out through the turbine to be increased. Thus, the vertical component of the flow also would be higher. Increasing this velocity component will increase the ventilation flow rate.

At a low Tip Speed Ratio (TSR), the blades of the turbine collide with the wind flow at a higher speed, equivalent to a higher wind speed at a constant rotational speed. This collision causes the wind flow coming out of the turbine to increase, including the vertical flow component, increasing the ventilation flow rate. As expected from the modeling section, the induction coefficient in the downwind is higher than the upwind, causing the flow velocity in the downwind to decrease more relatively.

Figure 13 illustrates the axial flow velocity, demonstrating different free-stream velocities in the upwind and downwind, concluding the stall velocity in both regions to be different. Therefore, the upwind rotor blades would experience a stall at lower wind speeds, while the downwind blades would encounter stall at

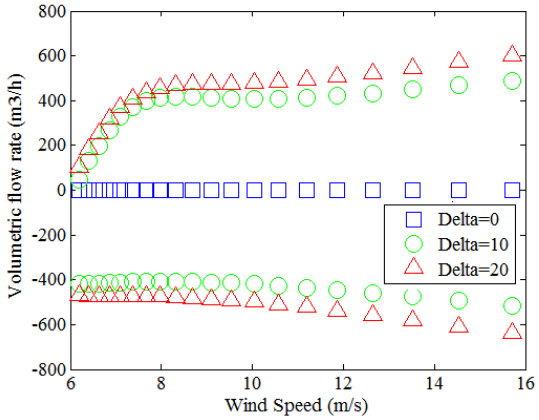

Figure 12. Diverted flow from the turbine (negative values for upwind and positive values for downwind)

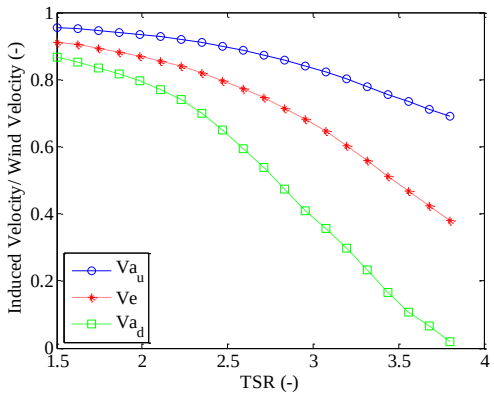

Figure 13. Wind speed at upwind and downwind at $\delta = 20^{\circ}$

higher wind speeds. This result, together with Figure 12, explains why the downwind curves are asymptotic. The amount of ventilation in the downwind phase increases within a range up to 7 m/s with a relatively high slope. After that, the blades enter the stall region, and consequently, flow enhancement is attenuated. The same profile occurs in the upwind, except that the stall velocity for upwind is less (about 5 m/s).

Figure 14 shows the Q-blade simulation for a cone angle of 20 degrees, a wind velocity of 8 m/s, and a tip speed ratio of 3. Separating the up and down current would enhance the ventilation process and establish a desired cycle within a room. The amount of flow diverted in the downwind phase is close to the upwind, except for the direction of the diverted flow.

To achieve a tradeoff between maximum power absorption and maximum ventilation, it is necessary to consider the type of use. According to Figures 10 and 12, wind speed around 10 m/s can be declared as a suitable point for absorbing power and ventilation. At high tip speed ratios corresponding to lower wind velocities, the flow downwind may be blinded due to the difference in flow velocity. Angling the blades reduces the power, and therefore, it is necessary to create a balance between power absorption and ventilation.

5. PARAMETRIC STUDY OF POWER AND VENTILATION COEFFICIENT

To achieve a downward relative flow rate for ventilation purposes, the diverted flow rate along the turbine axis should be normalized relative to the free-stream flow entering the rotor. This normalized quantity can be referred to as the ventilation coefficient. Figure 15 depicts changes in the ventilation coefficient for various conical angles in terms of the blade tip speed ratio. Both axes are dimensionless and can be generalized appropriately. Generally, it can be observed that the ventilation coefficient increases with the tip speed ratio. For instance, at a tip speed ratio of 3, approximately 2.5% of the flow entering the turbine vertically comes out from the upwind and downwind phases of the rotor. Assuming constant turbine angular velocity, the ventilation coefficient increases as wind speed decreases. The stall area for the upwind and downwind phases of this blade occurs at tip speed ratios of 5 and 3, respectively. At low tip speed ratios (high wind speeds), rotor blades enter the stall, leading to a decrease in relative performance but an increase in the diverted flow due to drag force effects. The ventilation coefficient initially increases with the tip speed ratio until a maximum is reached, corresponding to the stall vicinity point. After that, it decreases due to low wind speed.

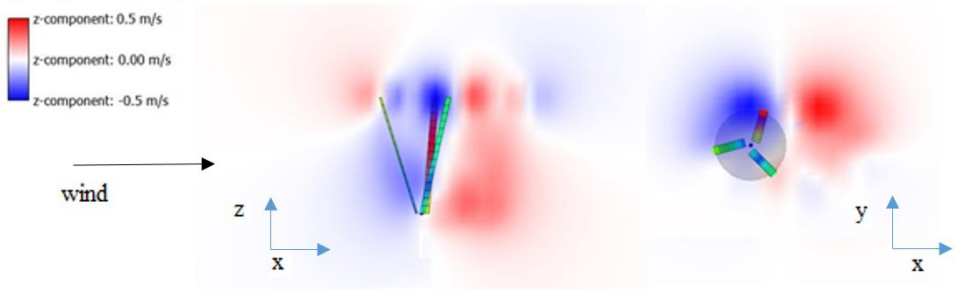

Figure 14. Flow velocity gradient along the turbine axis (Z-axis)

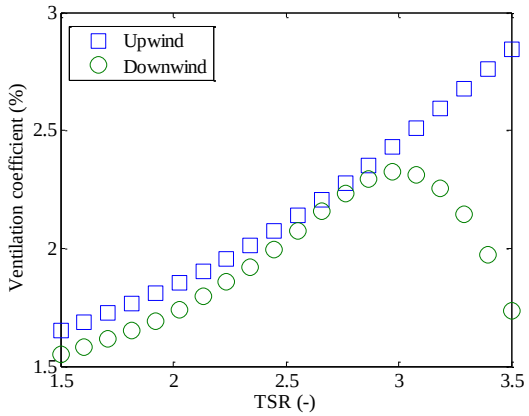

Figure 15. Downward flow rate (ventilation coefficient) at $\delta = 20^{\circ}$

As shown in Figure 12, low tip speed ratios always increase the ventilation flow. Conversely, Figure 15 indicates that reducing the tip speed ratio will decrease the ventilation coefficient due to stall. To achieve optimal performance from a ventilation perspective, a speed range of 8 m/s and a tip speed ratio of 3 can be used in this special turbine. This design point is suitable for both power and ventilation. Increasing the tip speed, would reduce the downward flow of the entire rotor and thus the ventilation coefficient and conversely, reducing tip speed, would result the turbine blades experiencing stall, leading to a degradation of both the ventilation and the power coefficients. The same argument can be drawn in terms of the tangential and normal force components.

Figure 16 shows the maximum turbine power coefficient at different cone angles. It can be observed that the maximum power coefficient decreases with increasing conical angle. From a conical angle of 15 degrees, the power coefficient experiences a local minimum. It would slightly be increased at higher conical angles, i.e., 20 degrees. This issue is partly related to the power coefficient definition. Applying a conical angle reduces the turbine power (similar to Figure 10) while simultaneously reducing the swept area introduced by this new geometry. At high conical angles, the rate of reduction of turbine power is lower than the rate of wind power reduction. As a result, the power coefficient slightly increases on the right side of the axis (larger conical angles).

Figure 17 shows the ventilation coefficient or relative flow rate plotted against cone angle variation, computed using the TSR averaging scheme. The plot indicates a nearly linear behavior in terms of the cone angle, suggesting that increasing the cone angle can improve ventilation efficiency. Additionally, the difference between the ventilation coefficient in the upwind and downwind could be increased with the cone angle, which is expected due to lower suction efficiency in the downwind section. However, this does not significantly affect ventilation performance.

In summary, Table 2 compares the performance of the turbine at different cone angles in terms of both power and ventilation. The table shows that increasing the cone angle decreases annual energy production as well as the maximum turbine power coefficient, while increasing the average ventilation coefficient. The challenge is to find a compromise between these two objectives. Since the maximum power is achieved at a TSR of about 3, the table also addresses the ventilation performance corresponding to the optimal TSR.

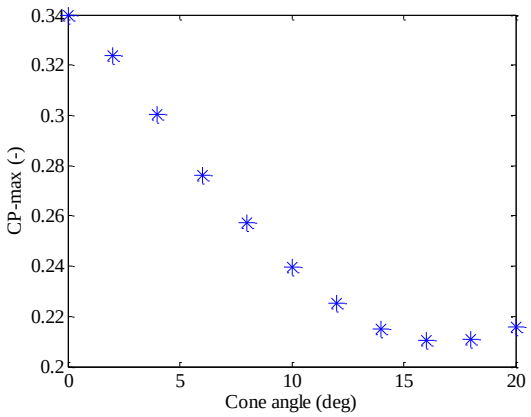

Figure 16. The relation between the maximum power coefficient and cone angle

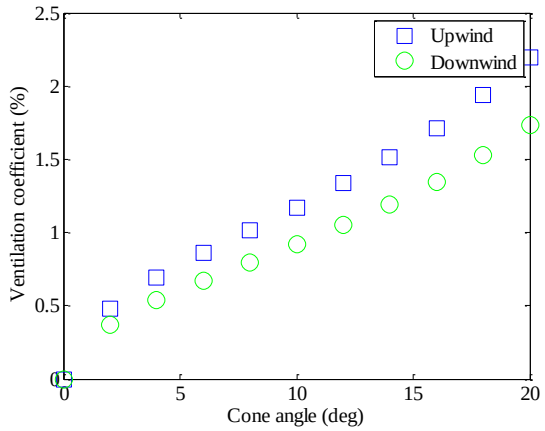

Figure 17. Equation of the average ventilation coefficient to the cone angle

According to the argument mentioned in the previous section, the optimal tip speed ratio from the power curve point of view was shown to be in the range of TSR=2.6 to TSR=2.8 (Figure 11). The maximum power coefficient will be achieved in this range of TSR in terms of cone angle selection. It is interesting that having the ventilation point of view, also the optimum TSR interval is 2.9 to 3.1 (Figure 15). It shows that a matching between the essential operation conditions for two objectives could be established. The required TSR for both power and ventilation coincided in the vicinity of TSR=3. Therefore, along with finding a suitable operating point, the TSR=3 is shown to be justified. Another design parameter to be selected is the cone angle. Considering the possible variation in the angular velocity of the rotor and the geometry, it would be suggested as 10-20 degrees range. The turbine can approach this suitable operating point in the range of wind speed between 4 m/s and 10 m/s by adjusting the RPM of the turbine.

TABLE 2. Comparison of turbine power and ventilation indicators

Cone angle (deg)	Max power (W)	AEP ($kW.h$)	Max power coefficient (%)	Upwind average ventilation factor (%)	Downwind average ventilation factor (%)	Upwind ventilation flow rate at TSR=3 (m^3/h)	Downwind ventilation flow rate at TSR=3 (m^3/h)
0	215	660	34	0	0	0	0
10	90	295	24	1.1	1	410	400
20	52	185	21	2.1	1.9	480	450

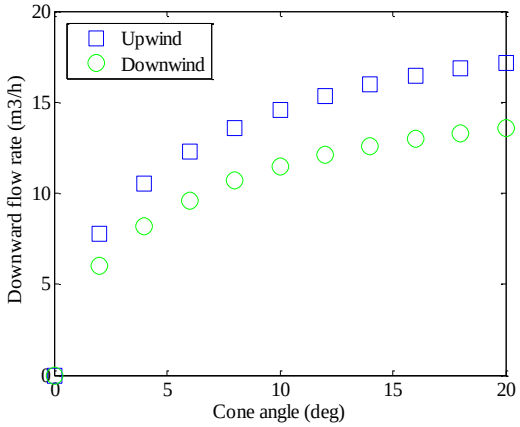

Figure 18. Equation of the average ventilation to the cone angle

Comparing the amount of ventilation in the three different cone angles for the optimal tip speed ratio, it is observed that the relative ventilation enhancement at a cone angle of 20 degrees compared to 10 degrees, is lower than the same difference for 10 degrees and zero (Figure 18). On the other hand, the power attenuation for a cone angle change from 20 to 10 is also less than the power loss for a change from 10 to 0. The relative progress in ventilation after cone angle 10 is lower than the relative penalty in the power for the same change in cone angle. Therefore, one may think that angle 10 is a suitable point for the two purposes. The power reduction in the 10-20 interval is more significant than the ventilation improvement, while it is vice versa for the 0-10 interval. Finally, it is concluded that the cone angle close to 10 degrees and the tip speed ratio of 3 (wind speed 7-9 m/s which was assumed a priori constraint of the target city) could be a good design point for the proposed turbine geometry in terms of both power generation and ventilation demand.

6. CONCLISION

The recent research presents a statistical survey of wind capacity for Manjil city in Iran based on the latest 3-year interval data. The territory exhibits an average wind velocity of 9.5 m/s, indicating a wind energy potential of 1000 W/m^2, as estimated from the wind probability curve. This makes it an ideal location for implementing home-scale wind turbines. The proposed turbine can yield an annual energy production of 600 kWh, 295 kWh, and 185 kWh for cone angles of 0, 10, and 20 degrees, respectively. Additionally, the implementation of the cone/inclined blade layout can lead to a further diversion or ventilation flow, suitable for internal circulation and cooling purposes. The addition of a baffle or vane can enhance the ventilation flow. By separating the inflow and outflow from the home, natural circulation can be maintained.

The inclined blade Darrieus-type turbine has a suitable power generation range of TSR=3 and higher, while the proper range of ventilation is TSR=3 and lesser. Therefore, operating the turbine at an optimum TSR of 3 would result in minimum penalties in power. The average flow entering the home can be adjusted up to 400 m^3/h, making it an adequate value for cooling during summer. Other findings from the semi-analytical code developed in the current research include:

1. The efficiency of the turbine decreases as the cone angle increases. For instance, the power coefficient at cone angles of 0, 10, and 20 degrees is 0.34, 0.24, and 0.21, respectively.
2. At a cone angle of 20 degrees and a TSR of 3, the ventilation coefficient is 2.5%.
3. The V-shaped turbine's average ventilation flow rate is 400 m^3/h.
4. The annual energy production at a conical angle of 10 degrees will be approximately half that of the H-shaped turbine, and at a conical angle of 20 degrees, it will be approximately one-third.

To improve the performance of home-scale wind turbines and satisfy power and ventilation needs, implementing a simple control mechanism is recommended. Changes should be made in the turbines' control system to ensure that their geometric characteristics are suitable for the weather conditions of the region. Further research can also be conducted on how to channel the flow under the turbine, as well as its proper position and geometry to efficiently absorb the diverted flow and bring it to the desired location.

7. REFERENCES

1. Kumar, A., Tausinga, S., Kishore, K., Nair, K. and Rao, D.K., "Technical and economic prospect of wind energy at lapaha, tonga", ***Resources and Environmental Economics***, Vol. 2, No. 1, (2020), 136-142. https://doi.org/10.1016/j.renene.2009.07.021
2. Mirhosseini, M., Sharifi, F. and Sedaghat, A., "Assessing the wind energy potential locations in province of semnan in iran", ***Renewable and Sustainable Energy Reviews***, Vol. 15, No. 1, (2011), 449-459. https://doi.org/10.1016/j.rser.2010.09.029
3. Alamdari, P., Nematollahi, O. and Mirhosseini, M., "Assessment of wind energy in iran: A review", ***Renewable and Sustainable Energy Reviews***, Vol. 16, No. 1, (2012), 836-860. https://doi.org/10.1016/j.rser.2011.09.007
4. Mostafaeipour, A., "Feasibility study of harnessing wind energy for turbine installation in province of yazd in iran", ***Renewable and Sustainable Energy Reviews***, Vol. 14, No. 1, (2010), 93-111. https://doi.org/10.1016/j.rser.2009.05.009
5. Mostafaeipour, A., "Economic evaluation of small wind turbine utilization in kerman, iran", ***Energy Conversion and Management***, Vol. 73, (2013), 214-225. https://doi.org/10.1016/j.enconman.2013.04.018

6. Mostafaeipour, A. and Abarghooei, H., "Harnessing wind energy at manjil area located in north of iran", ***Renewable and Sustainable Energy Reviews***, Vol. 12, No. 6, (2008), 1758-1766. https://doi.org/10.1016/j.rser.2007.01.029
7. Weigt, H., "Germany's wind energy: The potential for fossil capacity replacement and cost saving", ***Applied Energy***, Vol. 86, No. 10, (2009), 1857-1863. https://doi.org/10.1016/j.apenergy.2008.11.031
8. Eskin, N., Artar, H. and Tolun, S., "Wind energy potential of gökçeada island in turkey", ***Renewable and Sustainable Energy Reviews***, Vol. 12, No. 3, (2008), 839-851. https://doi.org/10.1016/j.rser.2006.05.016
9. Fyrippis, I., Axaopoulos, P.J. and Panayiotou, G., "Wind energy potential assessment in naxos island, greece", ***Applied Energy***, Vol. 87, No. 2, (2010), 577-586. https://doi.org/10.1016/j.apenergy.2009.05.031
10. Xydis, G., Koroneos, C. and Loizidou, M., "Exergy analysis in a wind speed prognostic model as a wind farm sitting selection tool: A case study in southern greece", ***Applied Energy***, Vol. 86, No. 11, (2009), 2411-2420. https://doi.org/10.1016/j.apenergy.2009.03.017
11. Paraschivoiu, I., Trifu, O. and Saeed, F., "H-darrieus wind turbine with blade pitch control", ***International Journal of Rotating Machinery***, Vol. 2009, (2009). https://doi.org/10.1155/2009/505343
12. Cheng, Q., Liu, X., Ji, H.S., Kim, K.C. and Yang, B., "Aerodynamic analysis of a helical vertical axis wind turbine", ***Energies***, Vol. 10, No. 4, (2017), 575. https://doi.org/10.3390/en10040575
13. Zanforlin, S. and Deluca, S., "Effects of the reynolds number and the tip losses on the optimal aspect ratio of straight-bladed vertical axis wind turbines", ***Energy***, Vol. 148, (2018), 179-195. https://doi.org/10.1016/j.energy.2018.01.132
14. Rasekh, S., Hosseini Doust, M. and Karimian, S., "Accuracy of dynamic stall response for wind turbine airfoils based on semi-empirical and numerical methods", ***Journal of Applied Fluid Mechanics***, Vol. 11, No. 5, (2018), 1287-1296. https://doi.org/10.29252/jafm.11.05.28668
15. Karimian, S. and Rasekh, S., "Power and noise performance assessment of a variable pitch vertical axis darrieus type wind turbine", ***Journal of the Brazilian Society of Mechanical Sciences and Engineering***, Vol. 43, No. 9, (2021), 437. https://doi.org/10.1007/s40430-021-03103-4
16. Moghimi, M. and Motawej, H., "Developed dmst model for performance analysis and parametric evaluation of gorlov vertical axis wind turbines", ***Sustainable Energy Technologies and Assessments***, Vol. 37, (2020), 100616. https://doi.org/10.1016/j.seta.2019.100616
17. Sedaghat, A., Assad, M.E.H. and Gaith, M., "Aerodynamics performance of continuously variable speed horizontal axis wind turbine with optimal blades", ***Energy***, Vol. 77, (2014), 752-759. https://doi.org/10.1016/j.energy.2014.09.048
18. Sedaghat, A., Samani, I., Ahmadi-Baloutaki, M., Assad, M.E.H. and Gaith, M., "Computational study on novel circulating aerofoils for use in magnus wind turbine blades", ***Energy***, Vol. 91, (2015), 393-403. https://doi.org/10.1016/j.energy.2015.08.058
19. Li, L. and Mak, C.M., "The assessment of the performance of a windcatcher system using computational fluid dynamics", ***Building and Environment***, Vol. 42, No. 3, (2007), 1135-1141. https://doi.org/10.1016/j.buildenv.2005.12.015
20. Chong, W.-T., Muzammil, W.K., Wong, K.-H., Wang, C.-T., Gwani, M., Chu, Y.-J. and Poh, S.-C., "Cross axis wind turbine: Pushing the limit of wind turbine technology with complementary design", ***Applied Energy***, Vol. 207, (2017), 78-95. https://doi.org/10.1016/j.apenergy.2017.06.099
21. Adanta, D., Sari, D.P., Syofii, I., Prakoso, A.P., Saputra, M.A.A. and Thamrin, I., "Performance comparison of crossflow turbine configuration upper blade convex and curvature by computational method", ***Civil Engineering Journal***, Vol. 9, No. 1, (2023), 154-165.
22. Paraschivoiu, I., "Wind turbine design: With emphasis on darrieus concept, Presses inter Polytechnique, (2002).
23. Castelli, M.R., Englaro, A. and Benini, E., "The darrieus wind turbine: Proposal for a new performance prediction model based on CFD", ***Energy***, Vol. 36, No. 8, (2011), 4919-4934. https://doi.org/10.1016/j.energy.2011.05.036
24. Mohamed, M., "Performance investigation of h-rotor darrieus turbine with new airfoil shapes", ***Energy***, Vol. 47, No. 1, (2012), 522-530. https://doi.org/10.1016/j.energy.2012.08.044

Persian Abstract

چکیده

در تحقیق حاضر، یک توربین بادی محور عمودی نوین ارائه شده که توانایی ایجاد تهویه ضمن تولید انرژی را دارا است. ایده این روش از بادگیرهای باستانی گرفته است.در این مطالعه ابتدا ظرفیت باد شهر منجیل در ایران مورد بررسی قرار گرفته و یک توربین بادی معمولی در مقیاس خانگی متناسب با اقلیم این شهر ارزیابی شده است. برای طراحی هندسه توربین از یک کد نیمه تحلیلی سه بعدی بر اساس تئوری دابل مولتیپل استریم تیوب یا به اختصار دی ام اس تی استفاده شده است. تجزیه و تحلیل اعتبار سنجی روش حل نیز توسط توربین مرجع انجام شده است. با استفاده از این کد، عملکرد توربین شامل شاخص ضریب توان و انحراف جریان بررسی شده است. همچنین تأثیر زاویه مخروطی پره بر ضریب توان و تهویه مورد بررسی قرار گرفته است. نتایج این مطالعه پارامتر نشان می‌دهد که برای محدوده بهینه نسبت سرعت نوک پره ۲.۹–۳.۲ و با زاویه مخروطی ۲۰ درجه پره بر اساس منحنی توان، امکان تولید جریان تهویه تا ٤۰۰ متر مکعب در ساعت و توان خروجی ۵۰–۲۰۰ وات وجود دارد که این میزان معادل ۲.۵٪ از کل جریان ورودی به روتور است. همچنین مشاهده شد که در صورت استفاده از هندسه متناسب با اقلیم منطقه، می‌توان افت توان را کاهش داد. در نهایت، برخی از روندهای تعمیم یافته توابع هدف نیز بیان شده و می‌توان از این روش برای حل مشکلات جاری در حوزه انرژی و تهویه مطبوع استفاده کرد.